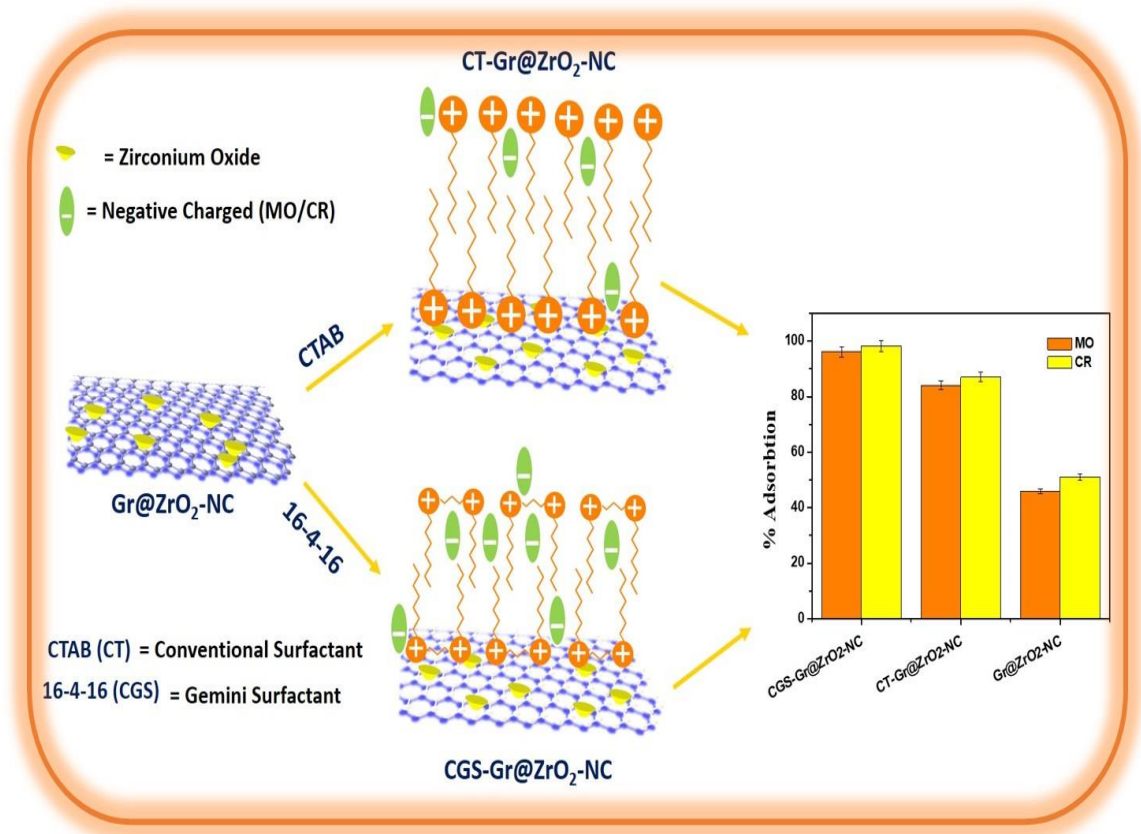


Chapter 3

Adsorption of Anionic Azo-Dyes Using Surfactant Modified Synthetic and Natural Adsorbents



3.1. Introduction

Textile waste, containing dyeing material, is a prime issue of concern for the environmental point of view [1-3]. This problem has been addressed by various treatment methods involving surfactants [4-17]. Among these treatments, adsorption is frequently studied and applied due to its effectiveness and ease of methodology. Both natural and synthetic adsorbents have received due attention for the dye adsorption process from the aqueous matrices [17, 18]. Well, known adsorbent material (silica, activated carbon or alumina) have proved their efficacy in the removal of soluble organic dye from background aqueous solution. It has been reported that various bio-adsorbents could prove useful for the above removal [19, 20]. Various researches have been performed to explore the utilization of egg wastes [21, 22,]. Due to the porous nature of eggshell, it may be used as an effective adsorbent for heavy metals and organic compounds [23, 24].

In the last two decades, graphene also attracted many researchers employing with adsorption technique, because of its excellent properties and two-dimensional structure [25]. Graphene oxide (GO), highly oxidized form of graphene, can be considered among the most known composite material obtained from exfoliation of graphite. Researchers started to synthesize more effective graphene adsorbents making some modifications to initial structure, resulting in functionalized graphene composites [26-28]. Moreover, exfoliated graphene oxide can provide large negative charge density which can help in interacting with hydrophobic cationic moieties available in aqueous solutions. Recently, graphene composites have been reported for the eradication of various contaminants including dyes [18, 25-30]. Graphene composites are preferred due to the increase of porosity, surface area possibility of contaminant diffusion inside internal space, *etc* [31-34].

Adsorption has been found dependent on adsorbent structure functional group or surface charge. Therefore, the natural adsorbent may or may not be suitable for potential removal of organic adsorbate. Due to this fact, adsorbent surfaces are modified by other materials in order to facilitate overall removal process. The ionic surfactant can interact with different inorganic, organic and natural/biological moieties due to the presence of charged head groups in their molecular structure.

Nowadays, natural and synthetic adsorbents are modified by various surfactants to improve their performances in order to diminish contamination of hydrophobic material in soil and aqueous bodies [17, 18]. When surfactants are applied for the modification of adsorbent surfaces, they commonly arrange as monolayers or bilayer depending upon their solution concentration. This modification can potentially solubilize or immobilized hazardous hydrophobic materials into the three-dimensional architecture formed due to surface modification. It has been reported that gemini surfactant treated clay is more efficient than their conventional counter-parts [35, 36]. Cationic gemini surfactant (CGS) has also been used for the modification of silica and it was observed that the adsorption amount of hydrophobic compound is related to the number of hydrophobic chains in a typical gemini surfactant [37-38].

Color components are always unacceptable in aqueous bodies for any use. Therefore, colors or color components in wastewater have now been termed as a contaminant that requires to be treated before mixing in the discharge stream. The literature survey shows that surfactant can play an important role in the pollution remediation of aqueous body contaminated by dyeing component of the textile, leather, food, cosmetic, pulp and paper wastes among others [1, 39]. Not many studies are available on the application of cationic gemini surfactant (CGS) modified composite of graphene-zirconium oxide (CGS-Gr@ZrO₂-NC) for the removal of water-soluble dyes.

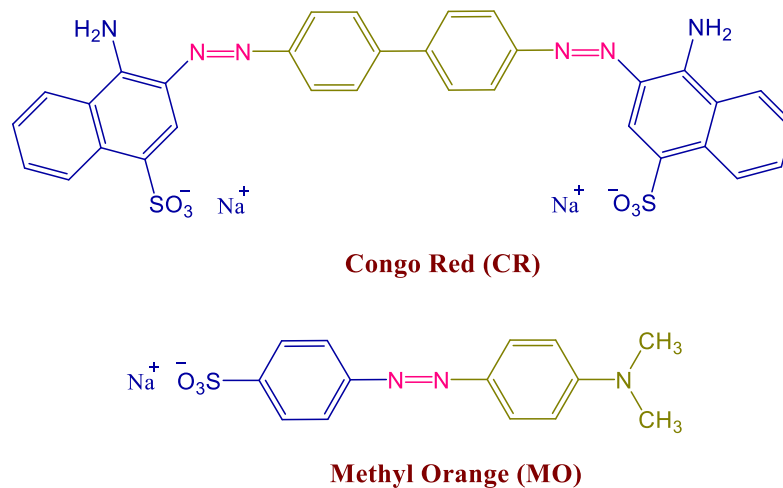
This inspired us to use CGS, *butanediyl-1,4, bis (N, N-hexadecyl ammonium) dibromide* (16-4-16) to modify Gr@ZrO₂-NC (CGS-Gr@ZrO₂-NC) and eggshell powder (EgSP) for the removal of anionic azo dyes (Methyl Orange, MO and Congo Red, CR) from aqueous system. The behavior was compared with a conventional cationic surfactant, *cetyltrimethylammonium bromide* (CTAB). CTAB is having the same alkyl chain length and generally used for the modification of adsorbents [40, 41].

3.2. Results and Discussion

3.2.1 Adsorption of Dyes on Surfactant Modified Adsorbents

Adsorption of anionic dyes (MO or CR, Scheme 1), from aqueous solution, were studied and relevant data are shown in Figures 1 (a & a'). A perusal of data indicates that modified composites perform better than the Gr@ZrO₂-NC or EgSP. The adsorption efficacy order was found: EgSP < CT-EgSP ~ CGS-EgSP < Gr@ZrO₂-NC < CT-Gr@ZrO₂-NC < CGS-Gr@ZrO₂-NC. This order may be decided by increased surface area (obtained by BET (Quantachrome, Quadrasorb SI) data (: 153.1; 181.4; 233.3, 16.3, 37.6 and 32.2. (m²/g) for Gr@ZrO₂-NC; CT-Gr@ZrO₂-NC, CGS-Gr@ZrO₂-NC, EgSP, CT-EgSP, and CGS-EgSP, respectively) and modified adsorbent surface charge. In addition to the above factors, a hydrophobic region (monolayer or bi-layer) may be available due to alkyl parts of surfactants which can facilitate adsorption of organic material (e.g., MO or CR). Among the surfactant-modified adsorbents, one with CGS was found even more effective than the CTAB modified one. This may be due to the presence of an additional hydrophobic tail/positively charged head group in CGS which may result more hydrophobically charged (+ve) composite surface which can interact with anionic dye moieties (of MO or CR). However, CT-EgSP and CGS-EgSP were found less effective adsorbent for CR (Figure 1b). Since these two adsorbents performed with similar efficacy hence CT-EgSP has been chosen

(to economize the process) for comparative adsorption studies with CGS-Gr@ZrO₂-NC.



Scheme 1. Representative chemical structures of anionic dyes methyl orange (MO) and congo red (CR)

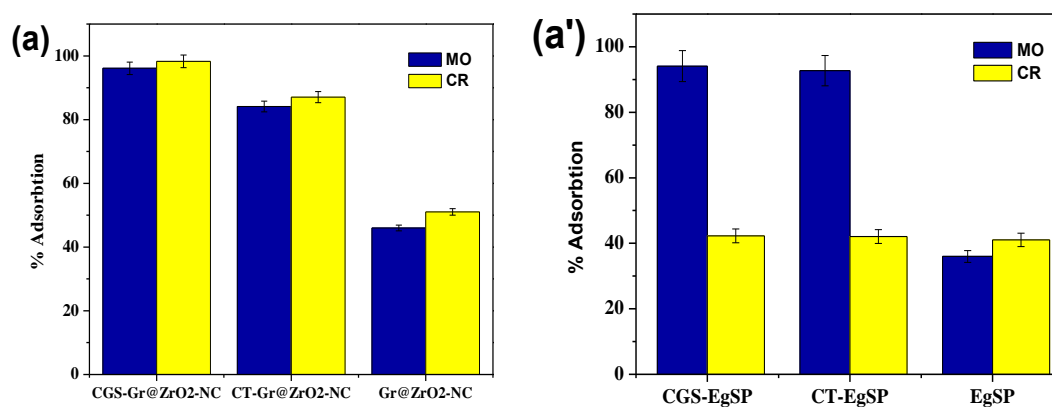


Figure 1. Percent adsorption of anionic azo dyes (MO and CR) on adsorbents with and without surfactant functionalization (a) Gr@ZrO₂-NC and (a') EgSP.

3.2.2. Effect of Adsorbent Doses/ [Dye] on Adsorption

The interplay of adsorbent dose and [adsorbate] has been shown in Figure 2. Influence of adsorbent dose on dye adsorption was performed by adding different adsorbent contents. The data acquired are depicted in Figures 2(a & a'). The adsorption percentages of MO and CR varies in the range 53 -96 % and 58 – 98 % (for CGS-Gr@ZrO₂-NC) and 48-92% and 27-42 % (for CT-EgSP), respectively, as adsorbent doses increased from 0.05 to 0.2 g followed by a constancy (up to 0.3). Therefore, 0.2 g of adsorbent has been taken as an optimized dose for other studies. At fix 0.2 g of adsorbent, [dye] was varied to show (Figures 2 (b & b')) the maximum capacity of the optimized dose to accommodate adsorbate moieties. Interestingly, dye adsorption shows a broad-maxima (~ 50 mg/L) followed by a distinct decrease on the continuous increase of [dye]. It can be interpreted in terms of constant cationic charge and hydrophobic volume resulted from the electrostatic binding of surfactant (CTAB or 16-4-16) on the composite surface. If this is correct, fixed dose of the adsorbent can bind anionic adsorbate (MO/CR) and then the presence of more adsorbate may create electrostatic repulsion between additional dye molecules of negative charges. Above discussion allows to say that adsorbate molecules in later stages (higher [dye]) would repel bulk molecules and responsible for decreased adsorption [42]. This indeed was observed in Figures 2 (b & b'). It has been observed that CR shows less response towards adsorbent (particularly with CT-EgSP), therefore, this adsorbent is only used for MO.

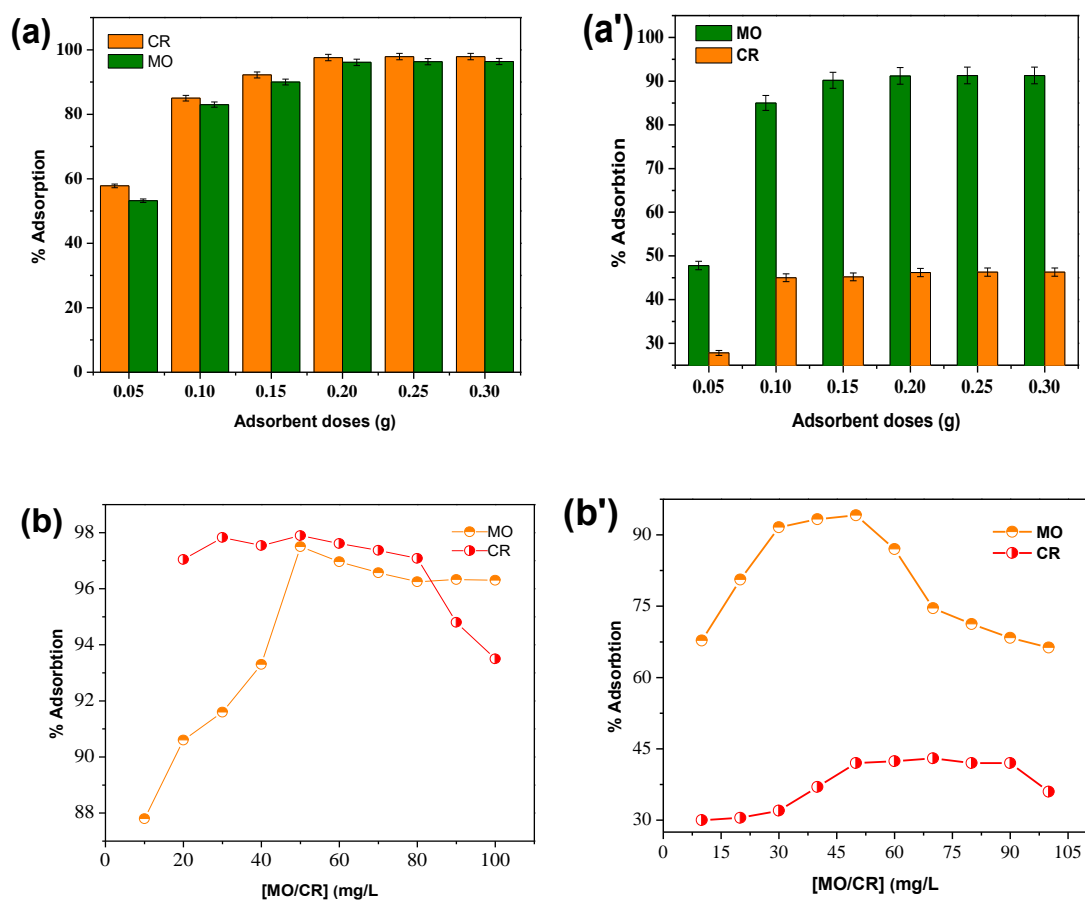


Figure 2. (a & a') Variation of percent adsorption of anionic azo dyes (MO and CR) with different dosages (in 20 ml) of CGS-Gr@ZrO₂-NC and CT-EgSP (b & b') with different [dye] (mg/L) having a fixed dose (0.2 g/ 20ml) of CGS-Gr@ZrO₂-NC and CT-EgSP.

3.2.3. Effect of Contact Time and Initial MO/ CR Concentration

Adsorption data of dyes (MO/CR), at various initial concentrations (10, 50 or 1000 mg/L), with different time intervals are given in Figures 3(a-c). Data stat that as the initial [dye] increases both equilibrium time and equilibrium adsorption capacity (q_e) also increases. However, the effect could not be studied with 1000 mg/L in the system: CT-EgSP (since MO shows decreased adsorption even with 100 mg/L initial concentration). For CR, all the curves (Figure 3c) have the nearly the same character

(as for MO, Figure 3b), showing faster adsorption of CR within few minutes (< 5 m) and then equilibrium is attained. This shows the versatility of the CGS-Gr@ZrO₂-NC. Adsorption time was found much larger (1h) for another natural adsorbent [43]. Moreover, the adsorption time of our versatile adsorbent is nearly matched with an ionic liquid graphene sponge though different adsorbate was used [44]. However, higher equilibrium time ($\cong 5$ m) was observed in this case of MO (Figure 3b). The above trend was followed even with higher concentration of adsorbate (1000 mg/L) with an equilibrium time within 25 ± 2.5 m (Figure (3 b & c)). Further, when MO and CR were allowed to adsorb simultaneously, equilibrium time was near to the individual equilibrium time for each dye. This qualitative data (Figure 4) suggest that gemini modified adsorbate (CGS-Gr@ZrO₂-NC) can be applied for the adsorption of a mixture of dyes as reported in an earlier study [45]. At equilibrium, 85 ± 10 % adsorbate has been adsorbed which is showing good adsorbate-adsorbent combination. However, a detailed study needed with another adsorbate(s) to generalize the above observation. This may be mentioned here that molecular structural differences of two dyes and their interactions with composite would govern the overall process.

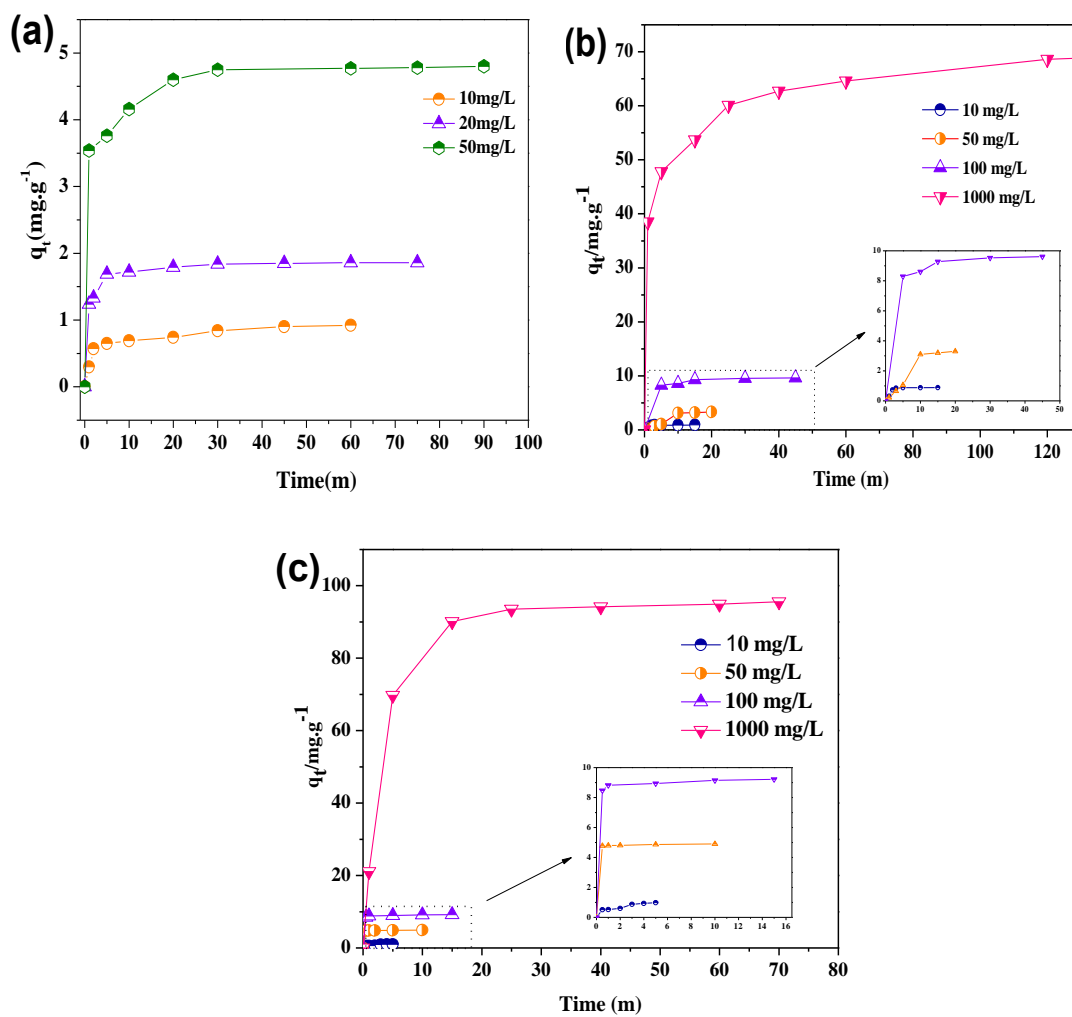


Figure 3. Variation of adsorption capacity (q_t) with time for Methyl Orange (a & b) CT-EgSP and CGS-Gr@ZrO₂-NC respectively. (c) For Congo Red with CGS-Gr@ZrO₂-NC.

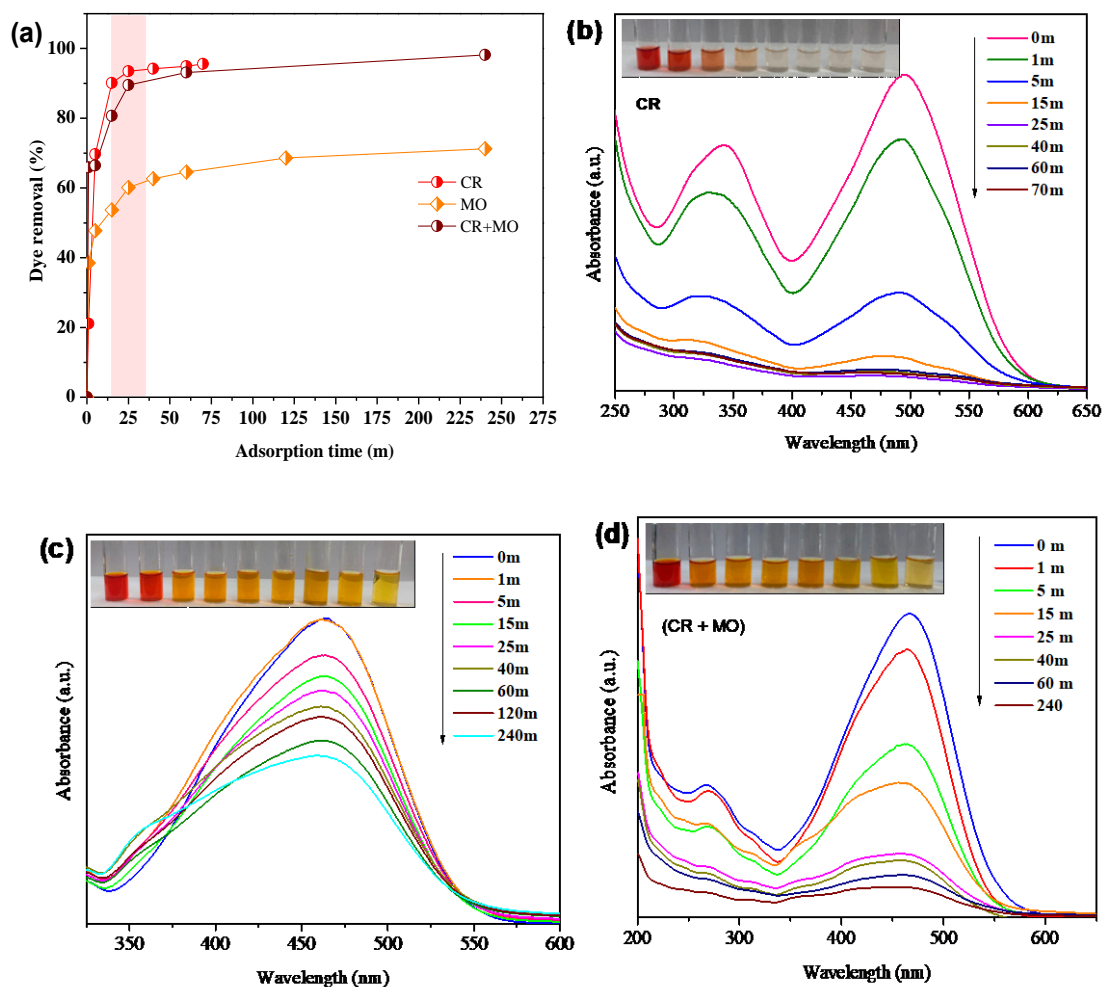


Figure 4. Variation of dye removal efficiency (initial [dye]= 1000mg/L), individual and mixed state, with time (a), UV- vis spectra of dyes (b and c) and their mixture (d) with time.

3.2.4. Effect of pH

The adsorption of dyes was found strongly dependent on the pH of the background solution (Figure. 5). The % adsorption was low in highly acidic conditions which increases with an increase in pH up to 3.0 followed by a near level off (pH = 3 to 10). Maximum dye adsorption ~3.0 pH may be due to the synergistic effect of coulombic, π - π stacking and van der Waals interactions. The adsorption of dyes with respect to pH can be explained in the light of surface charge on the modified adsorbent. At low pH,

the neutral form of dye will exist which only can adsorb on the surface hydrophobically. However, as the pH increases neutral form may decrease while negative dye molecule will increase. The latter effect seems responsible for the pH effect shown in Figure 5.

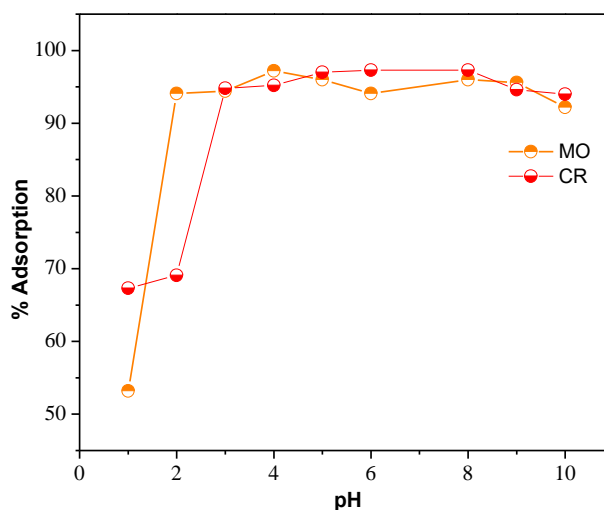


Figure 5. Effect of pH on percent adsorption of dyes.

3.2.5. Adsorption Isotherms

Data obtained by equilibrium adsorption experiments (Table 1) were analyzed in the light of different isotherm models [45-50]: Langmuir; Freundlich; Temkin and Dubinin–Radushkevich (D–R). The Langmuir isotherm can be represented by the eq. 1 as given below

$$\frac{1}{q_e} = \frac{1}{q_m} \times \frac{1}{b} \times \frac{1}{c_e} + \frac{1}{q_m} \quad (1)$$

where C_e is the equilibrium concentration of dyes in the solution (mg L^{-1}), q_e is the amount of dyes adsorbed per unit weight of adsorbent (mg g^{-1}), q_m is the amount of dyes required to form monolayer (mg g^{-1}) and b (L mg^{-1}) is a Langmuir constant related to energy of adsorption. The dependence of $1/q_e$ on $1/C_e$ with varying concentration of dyes was observed to be linear indicating the applicability of the Langmuir isotherm

(Figure 6a). The values of b and q_m were calculated from the slope and intercept of the linear plots of $1/C_e$ vs. $1/q_e$ [44,45]

The Freundlich isotherm represented by the following equation

$$\ln q_e = \ln K_f + \frac{1}{n} \ln C_e \quad (2)$$

Where K_f and n are Freundlich constants related to multilayer adsorption and adsorption intensity. The values of Freundlich isotherm constants K_f and n were calculated from the intercept and slope of the Freundlich plots at different temperatures Figure 6(b).

When 'n' approached zero, the surface site heterogeneity increased. The values of Temkin constants A and B related to adsorption potential and heat of adsorption respectively were calculated from the slope and intercept of the plot of q_e versus $\ln C_e$ Figure 6(c). The linear form of Temkin equation can be represented as

$$q_e = \left(\frac{RT}{b}\right) \ln A + \left(\frac{RT}{b}\right) \ln C_e \quad (3)$$

Or,

$$q_e = B \ln A + B \ln C_e \quad (4)$$

Where, $B = (RT/b)$, R is universal gas constant, T is absolute temperature and b is another constant.

To distinguish between the physical and chemical adsorption, Dubinin–Radushkevich (D–R) isotherm based on the heterogeneous nature of the adsorbent surface was applied. The linear form of this equation is represented as

$$\ln q_e = \ln q_m - K\varepsilon^2 \quad (5)$$

where ε is the Polanyi potential, q_m is the monolayer capacity (mol g^{-1}), K is a constant related to adsorption energy $\text{mol}^2/(\text{kT})^2$. The values of q_m (maximum adsorption capacity) and constant β were calculated from the intercept and slope of the D–R linear plots of $\ln q_m$ vs. ε^2 Figure 6 (d). The constant β gave an idea about the mean free energy

(E) (Kjmol^{-1}) of adsorption molecule of the adsorbate when it was transferred to the surface of the solid from infinity and can be calculated using the following relationship

$$E=1/(2\beta)^{1/2} \quad (6)$$

All the isotherm parameters computed from the above models are tabulated in Table 1. Based on the above discussion, both dyes adsorb *via* following the mechanism of monolayer adsorption on the surface of CGS-Gr@ZrO₂-NC.

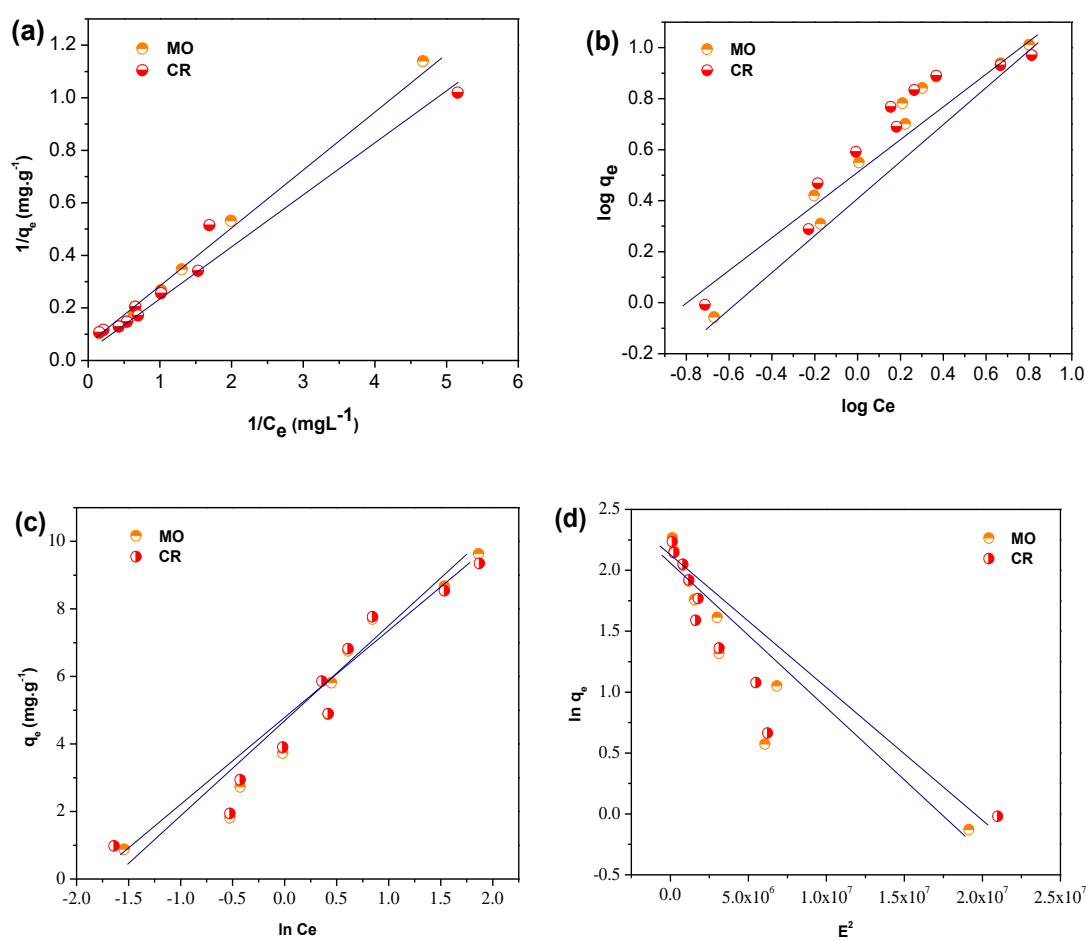


Figure 6. Isotherm of dyes adsorption by CGS-Gr@ZrO₂-NC (a) Langmuir, (b), Freundlich, (c) Temkin and (d) D-R isotherm.

Table 1. Isotherm data for adsorption of MO and CR on CGS-Gr@ZrO₂-NC.

Isotherms	parameters	Dyes	
		CR	MO
Langmuir	q _m	13.73	21.49
	b	0.387	0.197
	R ²	0.986	0.981
Freundlich	K _F	3.576	5.39
	n	0.675	0.528
	R ²	0.957	0.912
Temkin	A	7240	0.339
	B	0.012	0.014
	R ²	0.967	0.734
D-R	K	6.000	1.000
	q _m	0.65	6.94
	E	2182	2016
	R ²	0.805	0.830

3.2.6. Adsorption Kinetics

Pseudo-first order, Pseudo-second order, and intra-particle diffusion kinetic models were used to get insight into the rate of adsorption and adsorption kinetics. The pseudo-first order rate equation (eq. 7) of Lagergren [51] has been extensively used in relation to adsorption phenomenon. The simplified mathematical form of the equation can be written as

$$\log(q_e - q_t) = -\left(\frac{K_1}{2.303}\right) \times t + \log q_e \quad (7)$$

where q_e (mg g⁻¹) and q_t (mg g⁻¹) are the adsorption capacities at equilibrium and at time t , respectively. K_1 (min⁻¹) is the rate constant of the pseudo-first-order adsorption

process. K_1 can be calculated from the straight-line plots (Figure 7 a & a') between $\log(q_e - q_t)$ vs t by multiplying slope with 2.303 (Table 2). At a lower concentration (10 mg/L, Table 2) of MO, adsorption data with time reveals pseudo-first-order kinetics. However, the trend was not followed for higher [MO] as well as with CR (with all concentrations). This shows that the nature of the adsorption changes even with initial concentration and nature of the adsorbate.

But q_e calculated ($q_{e\text{ cal}}$) and q_e experimental ($q_{e\text{ exp}}$) differ appreciably indicating that pseudo-first-order kinetics is not the correct model to understand the adsorption process. This was the reason to apply other models in order to get an insight into adsorption kinetics. Pseudo-second order rate expression (eq. 4) can be represented as [52]

$$\frac{t}{q_t} = \frac{1}{K_2 q_e^2} + \frac{1}{q_e} \times t \quad (8)$$

where, K_2 ($\text{g mg}^{-1} \text{min}$) is the pseudo-second-order adsorption rate constant. Plots of t/q_t vs t (Figure 7 b & b') resulted in fairly good straight lines ($R^2 \cong 0.99$). q_e and K_2 were computed from the slope and intercept of the straight-line plots, respectively. The initial adsorption rate h ($\text{mg g}^{-1} \text{min}^{-1}$) was obtained by using equation 9 [53].

$$h = K_2 \times q_e^2 \quad (9)$$

Kinetic parameters for MO and CR, using pseudo-second-order rate law, are listed in Table 2. The validity of the experiment and kinetic model can be seen from the closeness of the values $q_{e\text{ cal}}$ and $q_{e\text{ exp}}$.

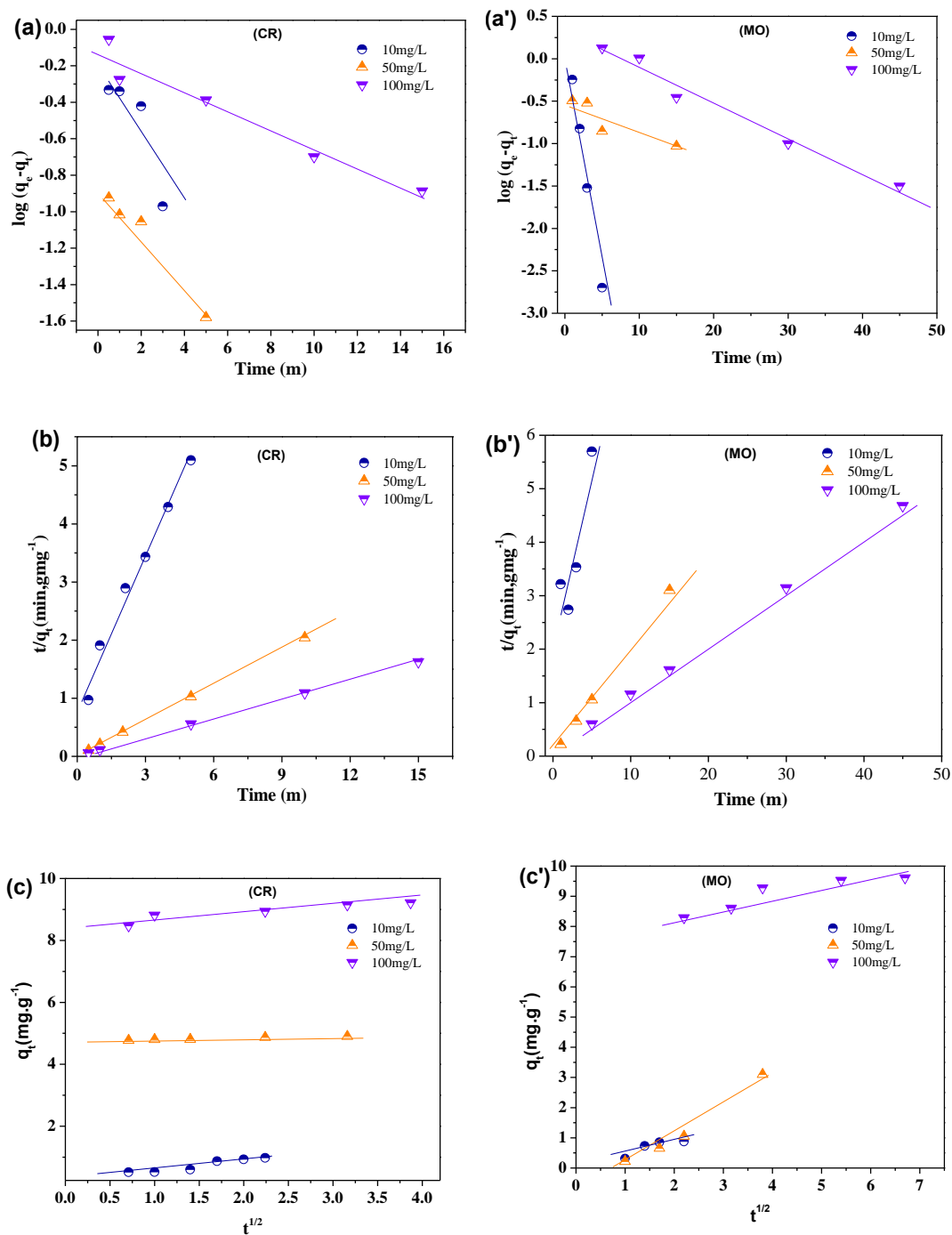


Figure 7. Pseudo first-order kinetics (a and a'), Pseudo-second order kinetics (b and b') and intra-particle diffusion model (c and c') for CR and MO adsorption on CGS-Gr@ZrO₂-NC at different [dye].

Kinetic data were also analyzed using the intra-particle diffusion model [54] and the relevant expressions and theory are given in supplementary information.

The plots of q_t vs \sqrt{t} are shown in Figure 7 c & c'. The values of K_{id} , I and R^2 are also listed in Table. 2 for MO and CR respectively. However, deviation in the plots from the origin (for all concentrations) hint that pore diffusion is not the sole rate-controlling mechanism. Probably, other processes like film diffusion may also contribute to the adsorption phenomenon. Looking at each kinetic model, one can easily decide about the validity of pseudo-second order.

Intra-particle diffusion

$$q_e = K_{id} \times t^{1/2} + I \quad (10)$$

where K_{id} ($\text{mg g}^{-1}\text{min}^{-1}$) is the intra-particle diffusion rate constant and I (mg g^{-1}) is a constant that gives an idea about the thickness of a boundary layer, q_t is the amount of dyes adsorbed (mg g^{-1}) at time t (min).

Table 2. Adsorption Kinetic Parameters for the adsorption of the MO and CR on CGS-Gr@ZrO₂-NC

Dye	Adsorbent (mgL ⁻¹)	q _{e(exp)} (mg g ⁻¹)	Pseudo- first order			Pseudo-second order				Intraparticle diffusion		
			q _{e(cal)} (mg g ⁻¹)	K ₁ (m ⁻¹)	R ²	q _{e(cal)} (mg g ⁻¹)	K ₂ (g/mg.m)	H (gmg ⁻¹ m ⁻¹)	R ²	K _{id}	C	R ²
MO	10	0.89	2.38	1.44	0.998	1.46	0.25	0.53	0.708	0.18	0.3	0.650
	50	4.87	0.32	0.09	0.729	3.98	2.36	37.3	0.999	1.05	1.0	0.963
	100	9.63	2.03	0.10	0.971	9.85	0.09	9.09	0.999	0.29	7.7	0.790
CR	10	0.98	1.31	0.57	0.691	1.18	0.72	1.01	0.979	0.35	0.2	0.893
	50	4.89	0.15	0.33	0.960	4.91	7.26	174.9	0.999	0.05	4.7	0.969
	100	9.35	0.74	0.12	0.934	9.24	1.36	116.0	0.999	0.2	8.5	0.830

3.2.7. Desorption Studies

To achieve the economy of the adsorption process, it is worthwhile to know the desorption process. This process has been carried out (Figure 8) by using several desorbing systems (0.01M HCl, 0.01M NaOH, Methanol, Ethylene glycol). Water and 0.01M HCl were nearly failed in desorbing the dye. However, 0.01M NaOH and methanol were able to desorb nearly 45% of the original adsorption. Maximum desorption (83 %) was achieved with ethylene glycol. This means polarity of the desorbing system has a role in recharging the adsorbent material.

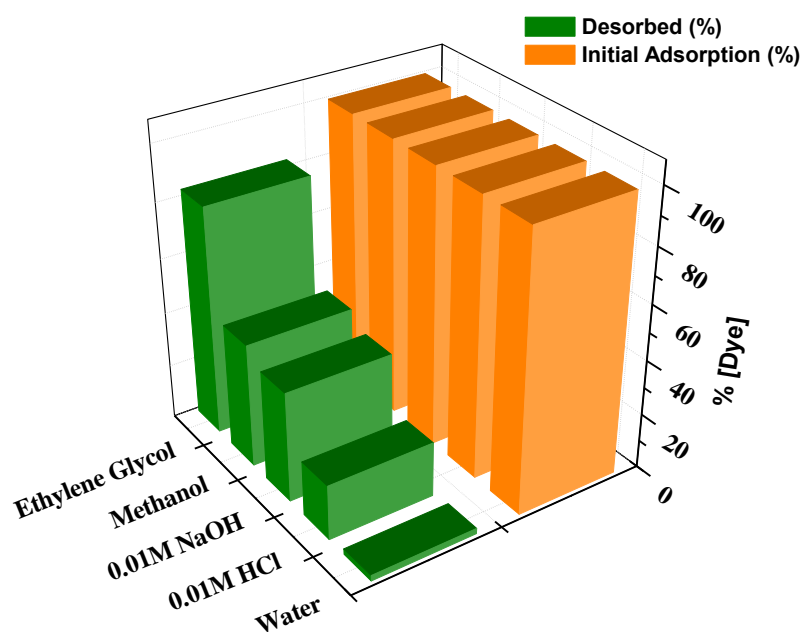


Figure 8. Desorption of dye (MO or CR) from CGS-Gr@ZrO₂-NC using different recharging solvent systems.

3.3. Conclusion

Surfactant functionalized natural and synthetic adsorbents CT-Gr@ZrO₂-NC, CGS-Gr@ZrO₂-NC, CT- EgSP and CGS-EgSP was synthesized and characterized. Adsorption behavior of all composites has been compared by taking MO and CR as adsorbates. Eggshell based adsorbents (both in natural and surfactant-modified form) were found inferior to Gr@ZrO₂-NC based adsorbents. Further, CGS-Gr@ZrO₂-NC has been found superior to CT-Gr@ZrO₂-NC (or CT-EgSP).

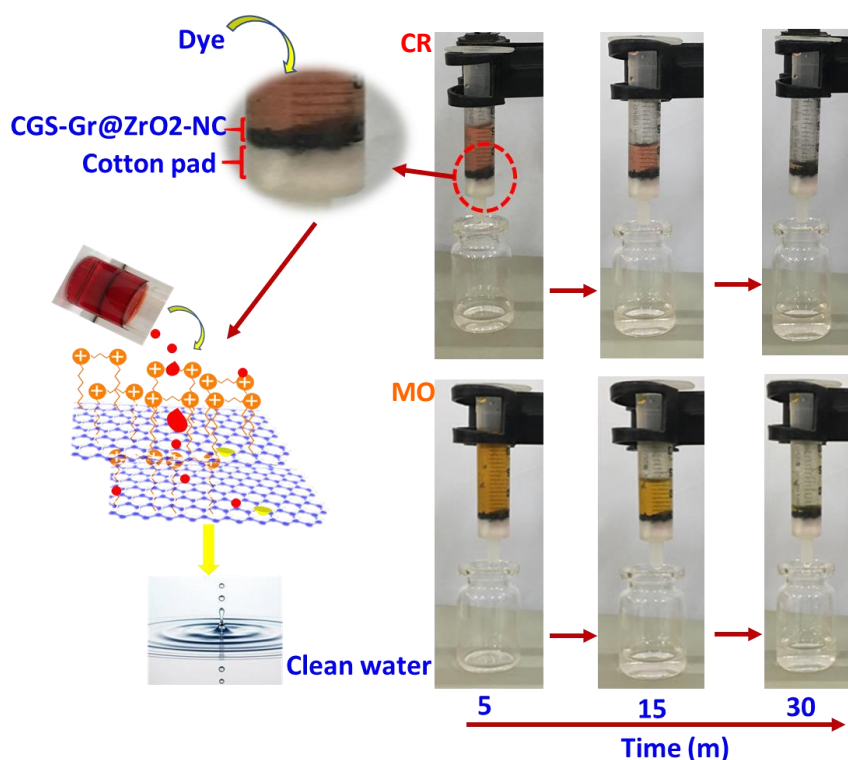


Figure 9. Proto type pictorial diagram for the auto-removal of dye (MO or CR) using CGS-Gr@ZrO₂-NC (< 0.5 cm) placed on the cotton pad.

Maximum adsorption, at equilibrium (~ 90 %), has been achieved within first 25 m of the contact indicating excellent absorptivity of the CGS-Gr@ZrO₂-NC for two structurally different anionic azo dyes whether present individually or simultaneously. The adsorption data followed Langmuir adsorption isotherm indicating that the surface of the adsorbent is homogeneous. Kinetic study showed that the pseudo-second-order

kinetic model has been obeyed. The re-usability of the adsorbent was demonstrated by desorbing the adsorbed dyes. Maximum desorption was achieved by using ethylene glycol. It has been seen that adsorbent when gently hold on a cotton pad (of thickness < 0.5 cm), shows nearly complete removal of each dye without interacting or leaving any colored spot on the pad (Fig.9). This information can be utilized in designing prototype filters to remove aqueous organic pollutants (dyes in particular) from the outlets of various industries.

References

- [1] M. Iqbal, *Chemosphere*, 2016, 144 785-802.
- [2] M. Iqbal, M. Abbas, M. Arshad, T. Hussain, A. Ullah Khan, N. Masood, M. Asif Tahir, S. Makhdoom Hussain, T. Hussain Bokhari, R. Ahmad Khera, *Pol. J. Environ. Stud.* 2015, 24.
- [3] M. Iqbal, J. Nisar, *J. Environ. Chem. Eng.* 2015, 3,1912-1917.
- [4] R. Dubey, J. Bajpai, A. Bajpai, *Journal of water process engineering*, 2015, 5. 83-94.
- [5] AU - Mahmoodi, Niyaz Mohammad, *Desalin. Water. Treat.* 2015, 53, 84-90.
- [6] N.M. Mahmoodi, M. Arabloo, J. Abdi, *Water Res.* 2014, 67, 216-226.
- [7] C.-H. Liu, J.-S. Wu, H.-C. Chiu, S.-Y. Suen, K.H. Chu, *Water Res.* 2007, 41, 1491-1500.
- [8] N.M. Mahmoodi, *J. Environ. Eng.* 2013, 139, 1368-1374.
- [9] W.-J. Lau, A. Ismail, *Desalination*, 2009, 245, 321-348.
- [10] N.M. Mahmoodi, B. Hayati, M. Arami, F. Mazaheri, *J. Chem. Eng. Data.* 2010, 55, 4660-4668.
- [11] N.M. Mahmoodi, *Ind. Eng. Chem.* 2015, 27, 251-259.
- [12] I. Bibi, N. Nazar, M. Iqbal, S. Kamal, H. Nawaz, S. Nouren, Y. Safa, K. Jilani, M. Sultan, S. Ata, *Adv. Powder Technol.* 2017, 28, 2035-2043.
- [13] M. Iqbal, I.A. Bhatti, *J. hazard. Mater.* 2015, 299, 351-360.
- [14] M. Iqbal, J. Nisar, M. Adil, M. Abbas, M. Riaz, M.A. Tahir, M. Younus, M. Shahid, *Chemosphere*, 2017, 168, 590-598.
- [15] N. Nazar, I. Bibi, S. Kamal, M. Iqbal, S. Nouren, K. Jilani, M. Umair, S. Ata, *Int. J. biol macromol*, 2018, 106,1203-1210.
- [16] M.A. Tahir, H.N. Bhatti, M. Iqbal, *J. environ.chem. eng*, 2016, 4, 2431-2439.
- [17] A. Kausar, M. Iqbal, A. Javed, K. Aftab, H.N. Bhatti, S. Nouren, *J. Mol. Liq.* 2018, 256, 395-407.
- [18] G.Z. Kyzas, E.A. Deliyanni, D.N. Bikiaris, A.C. Mitropoulos, *Chem. Eng. Res. Des.* 2018, 129, 75-88.
- [19] Arami, M., Limaee, N.Y., Mahmoodi, N.M. and Tabrizi, N.S. *J. Hazard. Mater.* 2006, 135, 171-179.
- [20] Sharma, P., Kaur, H., Sharma, M. and Sahore, V. *Environ. Monit. Assess.* 2011, 183, 151-195.

- [21] Chojnacka, K., 2005. *J. Hazard. Mater.* 121(1-3), 167-173.
- [22] Al-Ghouti, M.A. and Khan, M., *J. Environ. Manag.*, 2018, 207, 405-416
- [23] Wang, W., Chen, B. and Huang, Y., 2014. *J. Agric. Food Chem.* 62, 8051-8059.
- [24] B. Koumanova, P. Peeva, S.J. Allen, K.A. Gallagher, M.G. Healy, *J. Chem. Technol. Biotechnol.* 2002, 77, 539–545.
- [25] Z. Xu, C. Gao, *Acc. Chem. Res.* 2014, 47, 1267-1276.
- [26] S. Stankovich, D.A. Dikin, G.H. Dommett, K.M. Kohlhaas, E.J. Zimney, E.A. Stach, R.D. Piner, S.T. Nguyen, R.S. Ruoff, *Nature*, 2006, 442, 282.
- [27] E. Barjasteh, C. Sutanto, D. Nepal, *Langmuir*. 2019, 35, 2261–2269.
- [28] Y. Wang, X. Jiang, L. Zhou, C. Wang, Y. Liao, M. Duan, X. Jiang, *J. Chem. Eng. Data*. 2013, 58, 1760-1771.
- [29] N.M. Mahmoodi, S.M. Maroofi, M. Mazarji, G. Nabi-Bidhendi, *J. Surfactants and Detergents*, 2017, 20, 1085-1093.
- [30] G. Bhattacharya, S. Sas, S. Wadhwa, A. Mathur, J. McLaughlin, S.S. Roy, *RSC Adv.* 2017, 7, 26680-26688.
- [31] R.A.K. Rao, S. Singh, B.R. Singh, W. Khan, A. Naqvi, *J. Environ. Chem. Eng.* 2014, 2, 199-210.
- [32] B.R. Singh, M. Shoeb, W. Khan, A.H. Naqvi, *J. Alloys. Compd.*, 2015, 651, 598-607.
- [33] M. Kaur, K. Pal, *Int. J. Hydrog. Energy*, 2016, 41, 21861-21869.
- [34] L. Chen, J. Wang, M. Valenzuela, X. Bokhimi, D. Acosta, O. Novaro, *J. Alloys. comp.* 2006, 417, 220-223.
- [35] F. Li, M. Rosen, *J. Colloid Interf. Sci.*, 2000, 224, 265-271.
- [36] M. Rosen, F. Li, *J. Colloid. Interf. Sci.*, 2001, 234, 418-424.
- [37] K. Esumi, M. Goino, Y. Koide, *J. Colloid. Interf. Sci.*, 1996, 183 539-545.
- [38] A.M. Khan, F. Shafiq, S.A. Khan, S. Ali, B. Ismail, A.S. Hakeem, A. Rahdar, M.F. Nazar, M. Sayed, A.R. Khan, *J. Mol. Liq.* 2018 274, 673-680.
- [39] M.M. Ayad, A.A. El-Nasr, *J. Phys. Chem. C*, 2010, 114, 14377-14383.
- [40] Y. Wu, H. Luo, H. Wang, C. Wang, J. Zhang, Z. Zhang, *J. Colloid. interf. sci.* 2013, 394 183-191.
- [41] Y. Jin, F. Liu, M. Tong, Y. Hou, *J. Hazard. mater.*, 2012, 227, 461-468.
- [42] C.-Y. Kuo, C.-H. Wu, J.-Y. Wu, *J. Colloid. Interf. Sci.* 327 (2008) 308-315.
- [43] Z. Luo, M. Gao, Y. Ye, S. Yang, *Applied Surface Science*, 2015, 324, 807-816.

- [44] R. Zambare, X. Song, S. Bhuvana, J.S. Antony Prince, P. Nemade, *ACS Sus. Chem. Eng.* 2017, 5, 6026-6035.
- [45] I. Langmuir, *J. Am. chem. society*, 1916, 38, 2221-2295.
- [46] R. Say, A. Denizli, M.Y. Arica, *Bioresor. Technol.*, 2001, 76, 67-70.
- [47] H. Freundlich, *Chemie*, 1907, 57, 385-470.
- [48] W. Bouguerra, M.B.S. Ali, B. Hamrouni, M. Dhahbi, *Desalination*, 2007, 206, 141-146.
- [49] R.A.K. Rao, M.A. Khan, B.-H. Jeon, *J. hazard. mater.* 2010, 173, 273-282.
- [50] S.M. Hasany, M.H. Chaudhary, *Appl. Radiat. Isot.* 1996, 47, 467-471.
- [51] H. Yuh-Shan, *Scientometrics*, 2004, 59, 171-177.
- [52] Y. Ho, G. McKay, *Can. J. Chem. Eng.*, 1998, 76, 822-827.
- [53] Y.-S. Ho. *Water Research*, 2003, 37, 2323-2330.
- [54] R.A.K. Rao, S. Ikram. *Desalination*, 2011, 277, 390-398.